

**Zeitschrift:** Schweizer Ingenieur und Architekt  
**Herausgeber:** Verlags-AG der akademischen technischen Vereine  
**Band:** 101 (1983)  
**Heft:** 4

**Artikel:** Formation of the solar system from a potential-vortex-natured nebula disk. Part II: Disintegration of the swirling solar nebula disk into vortices of the infant planets due to selfexcited vibrations caused by the surface winds  
**Autor:** Chen, Yian N.  
**DOI:** <https://doi.org/10.5169/seals-75047>

### **Nutzungsbedingungen**

Die ETH-Bibliothek ist die Anbieterin der digitalisierten Zeitschriften. Sie besitzt keine Urheberrechte an den Zeitschriften und ist nicht verantwortlich für deren Inhalte. Die Rechte liegen in der Regel bei den Herausgebern beziehungsweise den externen Rechteinhabern. [Siehe Rechtliche Hinweise.](#)

### **Conditions d'utilisation**

L'ETH Library est le fournisseur des revues numérisées. Elle ne détient aucun droit d'auteur sur les revues et n'est pas responsable de leur contenu. En règle générale, les droits sont détenus par les éditeurs ou les détenteurs de droits externes. [Voir Informations légales.](#)

### **Terms of use**

The ETH Library is the provider of the digitised journals. It does not own any copyrights to the journals and is not responsible for their content. The rights usually lie with the publishers or the external rights holders. [See Legal notice.](#)

**Download PDF:** 14.05.2025

**ETH-Bibliothek Zürich, E-Periodica, <https://www.e-periodica.ch>**

kraftwerkes Angra 2 in Brasilien, die in [3] aufgeführt ist, kurz gestreift werden. Unterhalb der Fundamentplatte befindet sich der horizontal geschichtete Boden mit einer Stärke von 35 m, der auf Fels ruht. Die Foundation (Bild 7) besteht aus 202 Spitzenpfählen (146 mit Durchmesser 1,3 m, 56 mit Durchmesser 1,1 m) und 88 schwimmenden Pfählen mit einer Länge von 15 m (80 mit Durchmesser 1,8 m, acht mit Durchmesser 1,3 m). Die Erdbebenbeschleunigung von 0,1 g in horizontaler Richtung wirkt auf der Höhe des Felsens. Infolge der (approximativen) Symmetrie kann die Berechnung auf einen Viertel

beschränkt werden. Längs der Kontaktfläche zwischen den Pfählen und des Bodens werden 556 Knoten eingeführt (Bild 8), die auch die dynamische Steifigkeitsmatrix des Bodens festlegen. Als Beispiel der Resultate werden im Bild 9 die maximalen Querkräfte an den Pfahlköpfen dargestellt. Wie erwartet, werden die Pfähle am Rande stärker belastet (1,26mal den Mittelwert) als die im Zentrum (0,60mal den Mittelwert).

Adresse des Verfassers: Dr. J.P. Wolf, Elektrowatt Ingenieurunternehmung AG, Postfach, 8022 Zürich.

#### Zitierte Literatur

- [1] Wolf, J.P. und Weber, B. (1982): «On calculating the dynamic-stiffness matrix of the unbounded soil by cloning». Proceedings International Symposium on Numerical Models in Geomechanics, Zurich, A.A. Balkema (Rotterdam), pp. 486-494
- [2] Apsel, R.J. (1979): «Dynamic Green's Functions for Layered Media and Applications to Boundary-Value Problems». Ph. D. Dissertation, University of California, San Diego
- [3] Wolf, J.P., von Arx, G.A., de Barros, F.C.P. and Kakuba, M. (1981): «Seismic analysis of the pile foundation of the reactor building of the NPP Angra 2». Nuclear Engineering and Design, Vol. 65, No. 3, pp. 329-341

## Formation of the Solar System from a potential-vortex-natured Nebula Disk

### Part II: Disintegration of the swirling solar nebula disk into vortices of the infant planets due to selfexcited vibrations caused by the surface winds

By Yian N. Chen, Winterthur

Evaluation of the present orbits of the planets and the asteroid's leads to the discovery of the primordial solar system as a potential-vortex-natured nebula disk. The winds on its surfaces caused by the gravity of the infant sun, similar to the surface flows of a bath-tub vortex, would have induced a tidal wave pattern in the disk due to a kind of the self-excited vibration. This wave pattern would have become unstable owing to nonlinearity, with the result of its disintegration into vortices representing the primeval planets. It can be shown that the local values of the vorticity and the coriolis acceleration of the nebula disk will then determine the angular momentum of the future planet about its own axis. The orbits of the inner planets Mercury, Venus, earth and Mars, and those of the asteroid's, divided by the various Kirkwood gaps, correspond then to the nodal circles of the tidal-wave pattern, whilst the orbits of the outer planets Jupiter, Saturn, Uranus, Neptune and Pluto correspond to the anti-nodal circles of this pattern. It can be further shown that this difference in the orbital patterns and the density distribution of these planets are an expression of the surface winds mentioned.

#### Excitation of the tidal waves in the primordial gaseous disk of the solar system

The primordial gaseous disk of the solar system, as suggested in a previous chapter, is sketched in subfigure b of Fig. 11 corresponding to the present position of the planets and the asteroids (subfigure a). The disk represents a potential vortex superimposed on a gravitation field of a great mass  $M$  situated in the center of the disk. The disk of a dense mass rotates in a space of

a rather small density. The following flow model can be established from the *fluid-dynamic theory*:

A profile of the swirl velocities such as curve 1 can be supposed. In the boundary layer between the disk and the space, the swirl velocity  $v_\phi$  is much less than that in the disk ( $v_{\phi 0}$ ). The centrifugal force of the boundary layer can therefore not balance the gravity of the central mass  $M$ . A radial flow on the surface of the disk will be generated, as denoted by 2 in the outer planet field and by 2' in the inner planet field. On the other hand, the inflow (3) from the

zenithal direction will be generated by the gravitation of the mass  $M$ . This inflow, which will be strongly accelerated by approaching the central region, can be compared with a jet directed on a wall (Sketch in subfigure c).

In the central region (4), a very high pressure will be generated due to impact on the mass  $M$ . This high pressure center will deflect the flow outward (5) to stream within a thin layer over the surface of the gaseous disk. Due to strongly curved stream lines (5), the gaseous disk will be pressed tightly together in the region (6), until a deceleration 7 takes place over the further stretch 8. This outward flow will form a toroidal ring vortex with the inward flow 2' below it, much the same as on the bath-tub vortex (flows  $c$  and  $a'$  in Fig. 9). This toroidal ring vortex will increase the instability of the gaseous disk. However, the outward flow outweighs the inward flow, so that the effect of the latter on the surface of the gaseous disk will be masked by the former so far as their role as a surface wind is concerned. Fig. 11 a shows the variation of the radial velocities.

The outward flow of the inner field, will meet the inward flow (2) of the outer field at the position of Jupiter (9). The inward flow needs a much longer way to reach the same velocity as that of the outward flow in order to stop it. Therefore, Jupiter lies much nearer to the sun than to the outer edge of the gaseous disk.

The huge amount of gas carried by these two flows will be piled up there so that a very thick gas ring will be formed separating the outer field from the inner one. The wind over the surface of the inner field is very strong at the beginning along

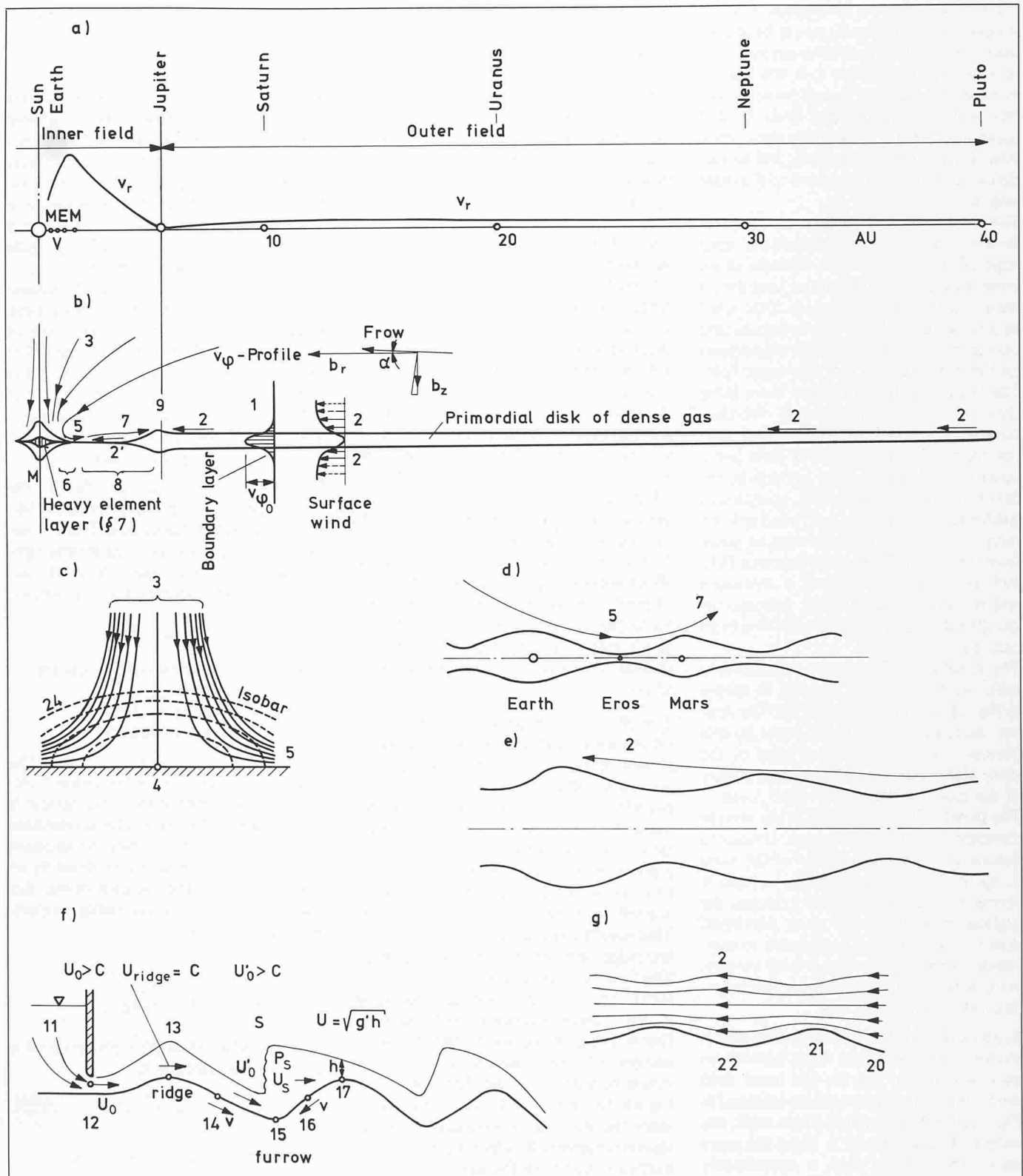


Fig. 11. Generation of surface winds on and tidal waves in the primordial nebula disk of the solar system

a) Velocities of the surface winds versus distance  $r$ , blowing outward over the inner field, but blowing inward over the outer field.

b) & c) Wind pattern of the flow model.  
1 swirl velocity profile of the rotating gaseous disk, 2 surface wind over the outer field (with profile), 3 jet-like inflow over the cen-

tral mass  $M$  (i.e. the Sun), 4 central stagnation region of the jet-like inflow, 2', 5, 7 surface winds over the inner field, 6 region of the gaseous disk tightly pressed by the inflow, 8 region of decelerated surface wind 7

d) Outward surface wind over the tidal wave of the inner field

e) Inward surface wind over the tidal wave of the outer field

f) Stormy surface wind over a wavy weir as a model for the wave generation in the inner field (Oswatitsch & Wiegardt 1965)

g) Mild surface wind over a wavy weir as a model for the wave generation in the outer field.

the stretch 6. It then decelerates down to stagnation at position 9, as will be shown later. The stretch 6 is not only pressed very thin by the curved flow 5, it will also be very dense, because heavy particles like dust will be centrifugalized from the said curved flow into it. Most of the light gases, such as hydrogen and helium, will be carried away by this surface wind to the huge ring 9.

The wind over the surface of the outer field is very weak at its origin of the outer edge of the gaseous disk because of its great distance from the center, and thus a weak gravitational force there. This wind in a rather thick layer will be accelerated during travelling inward, until it is stopped by the outward flow 7 of the inner field. The impact of these two flow there bring their radial components to rest. We thus have a rather stormy wind within thin boundary layer over the inner field and a much milder wind within a thick boundary layer over the outer field, as shown in subfigures d and e. This mild wind will not carry away to much of the original gases from the disk surface so that the outer field will remain rich in gases (i. e. hydrogen and helium), whose content increases in the direction of the surface wind due to its carrying effect.

The distribution of the density of the planets with the distance from the sun, as shown in Fig. 12, can thus be explained. The density decreases first from the inner planets Mercury, Venus, earth and Mars to the giant planet Jupiter, due to carrying away of the gases by the stormy wind 5 and 7. The density decreases again in the reverse direction from Pluto, Neptune, Uranus to Saturn due to the same effect of the wind 2. As the density of Saturn is the least, it seems that the surface wind 2 reaches the highest speed here and then decelerate down to position 9 of Jupiter due to stagnation caused by the impact with the outward wind 7 of the inner field, see the radial velocity  $v_r$  in Fig. 11a.

Suppose that the primordial gaseous disk is excited to show a tidal wave pattern, as sketched in Fig. 11d for the inner field with a thin, but stormy surface wind and in Fig. 11e for the outer field with a thick, but mild surface wind over it. Since the space above the surface wind is considerably void in matter compared with the wind and the gaseous disk, this wind can be considered as a flow of dense fluid over ridges and furrows of the wave pattern of the dense gas disk. We thus reduce the wind to a water stream over a wavy weir along a channel, as is shown in Fig. 11f and 11g for the inner field and the outer one, respectively. The following interaction between the water stream and the wavy weir can be supposed in the model of Fig. 11f according to the fluid-dynamic theory (K. Oswatich & K. Wieghardt 1965, pp. 84–86).

The reservoir 11 models the stagnation pressure 4 of the jet flow 3 (Fig. 11c). A high velocity  $u_0$  is produced at the narrow outlet 12, being larger than the local tidal-wave-travelling-speed  $c$  ( $c = (gh)^{1/2}$ ,  $g$  gravity acceleration,  $h$  height of water level). This flow models the stormy wind of a thin layer over the gaseous disk. The flow velocity will decelerate to  $c$  at the top of the ridge 13 and accelerate again to  $u'_0$  ( $> u_0$ ) during streaming downward the hang 14. A shock at approximately 15 will be generated in front of the following ridge 17 to reduce the flow velocity considerably under the value of  $c$ . At the top the ridge 17, the tidal-wave-travelling-speed will be reached again. Afterwards, the play described previously will repeat in the same manner.

Actually, the wavy weir represents the wave pattern of the gaseous disk. The positions 13, 15 and 17 denote the antinodal points of the vibrating pressure, and those 14 and 16 the nodal points of it. The high pressure  $p_s$  after the shock front  $s$  of the surface wind will help to lower the furrow 15 still more. This lowering effect of the shock pressure  $p_s$  increases with the depth of the furrow, once it exceeds a certain value to enable the formation of an effective shock front  $s$ . In this manner, a self-sustained vibration of the gaseous disk arises.

The effect of the mild wind of a thick layer on the wave pattern of the gaseous disk as shown in Fig. 11g for the outer field is somewhat different from that of the stormy wind in Fig. 11f for the inner field, because the wind velocity is smaller than the tidal-wave-travelling speed. The velocity pattern in Fig. 11g shows that the flow over the wave ridge 21 will be accelerated according to the fluid-dynamic theory. This acceleration causes a suction force on the ridge, thus reinforcing its amplitude. The flow over the furrow 22 will be decelerated, thus causing a stronger pressure on it. This stronger pressure will lower the furrow still more. In this manner, the wave pattern of the gaseous disk will be strengthened by the wind. The strengthening will be the more effective, the more violent the wave is. A feedback circle can thus be established, which leads to a self-excited vibration of the gaseous disk.

The two kinds of winds, the outward one through a thin layer with a high average velocity over the inner field, and the inward one through a thick layer with a low average velocity over the outer field can be supposed to have similar temperatures and thus similar viscosities. As the densities of the gases are also quite similar in these two gas flows, their *Reynolds numbers* will be of a similar order of magnitude. Since these two flows can be supposed to have the dynamic behaviour of a free-shear layer, they will possess quite similar *Strouhal numbers*

$S$  for the frequency  $f$  of the peak of each of their energy spectra:

$$(19) \quad S = f d / U$$

where  $d$  is the thickness of the wind layer and  $U$  is its mean velocity. If we suppose that the ratio of the mean wind velocities between the inner and the outer field were in the order of magnitude of 5, and the ratio of their wind layer thicknesses were in the order of magnitude of  $1/5$ , then the ratio of the frequencies of their energy peaks would be in the order of magnitude of 25.

The wind over the inner field will possess an energy density spectrum whose peak frequency will in the order of magnitude of 25 times higher than that of the wind over the outer field. We can thus expect that these winds will be capable of excitation of a high-frequent vibration on the inner field, and a low-frequent vibration on the outer field of the gaseous disk.

Fig. 11b shows that the outer field of the primordial gas disk gets thicker and thicker from its outer edge inward. The composition of the gas also gets lighter and lighter, but at a rather low rate. The gravity acceleration in the  $z$ -direction at any radius  $r$ :

$$(20) \quad b_z = 2\pi^2 \rho h G$$

(where  $h$  = thickness of the local gas layer,  
 $\rho$  = its average density,  
 $G$  = gravity constant)

will increase with the decrease of  $r$ . The gravity acceleration  $b_r$  in the radial direction must therefore work partly against  $b_z$  of the zenithal direction. The acceleration diagram in Fig. 11b shows the situation of a surface wind which is inclined by an angle  $\alpha$  owing to the increase of the disk thickness  $h$ . The effective, radial acceleration will reduce to

$$(21) \quad b_{r, \text{eff}} = b_r - b_z \operatorname{tg} \alpha = b_r \left\{ 1 - (b_z / b_r) \operatorname{tg} \alpha \right\}$$

As the radial acceleration is proportional to the following expression:

$$(22) \quad b_r \sim \frac{v_{\varphi 0}^2}{r} \sim \frac{(r v_{\varphi 0}^2)_{\text{outer edge}}}{r^2} \sim \frac{\text{const}}{r^2}$$

the ratio between  $b_z$  and  $b_r$  will be

$$(23) \quad b_z / b_r \sim \rho h G r^2$$

We suppose that the diameter  $d$  and the mean density  $\rho_{\text{planet}}$  of the planet formed from this primordial gas disk be proportional to  $h$  and  $\rho$  at the respective radius  $r$ . Then we may set

$$(24) \quad \operatorname{tg} \alpha = \frac{dd}{dr}$$

The correction in Eq (21) would be

$$(25) \quad (b_z / b_r) \operatorname{tg} \alpha \sim \rho_{\text{planet}} dr^2 \frac{dd}{dr}$$

The derivation of curve 1 for  $d$  (with somewhat scatter) supplies  $\tan \alpha$  as shown by curve 2, see Fig. 13. Using curve 3 for the expression  $\rho_{\text{planet}} dr^2$  we can finally calculate the correction mentioned as shown by curve 4. All these curves are made dimensionless by the corresponding values applied to the position of Jupiter. The corrections vary from 1 to 4,6 with the maximum value of 4,6 applied to Neptune. But, the absolute value of this maximum must be very small owing to the small thickness and the right flatness of the gas disk in the corresponding region. Thus such a correction will only bring a small increase of accuracy. We can therefore remain at our linear theory without considering the influence of the zenithal potential on the transfer of circulation brought about by the surface wind.

The pattern of the profile of the swirl velocities  $v_\phi$  of the primordial gas disk, as shown by curve 1 in Fig. 11b with the value decreasing from the central plane outward corresponding to a free shear layer, still remains in the distribution of the angular velocities of the sun at the present time. Its central plane rotates much faster than its outer region. Its equator rotates once every 25 days, whilst its pole rotates once about 34 days. The viscosity in the transition zones between equator and poles could disperse the rotation energy and then slow down the rotation speed of the sun. This theoretical inference can be verified using the following measurement results.

The Mount Wilson Observatory, California, headed by A. H. Vaughan, found in their measurements that the average chromospheric brightness is less for the more slowly rotating stars (N. Henbest 1981). These new measurements reveal that, when stars grow older, they rotate more slowly and their atmospheric activity decreases. This finding confirms other evidence that younger stars like those in the 300-million-year-old *Hyades cluster* have brighter chromospheric H & K lines than the sun which is 15 times older. The slowing-down of rotation of stars with age corresponds thus very well to the theory developed in the present paper.

## The wave pattern of the primordial gaseous disk of the solar system

The gaseous disk is symmetrical about its central plane 0-0 (Fig. 14a). The flow pattern in it will remain the same if we suppose that it is separated by a rigid wall, replacing this central plane according to the fluid-dynamic theory. We then have one half of the gaseous disk lying on a rigid ground (Fig. 14b). As the density of the

disk is considerably greater than that of the space over it, we can reduce the disk to a circular sea on our earth. This sea stays under the gravity field of the masses of itself. Whilst the radial component (in the direction  $r$ ) of this gravity field will keep the masses together against the centrifugal force, its axial component (in the direction  $z$ ) will be responsible for the generation of the tidal waves discussed in the previous chapter.

The gravity acceleration in the  $z$ -direction is determined by the local condition, namely:

$$(26) \quad g = 2\pi^2 \rho h G$$

as shown in the foregoing chapter. The travelling velocity of the tidal wave will be

$$(27) \quad c = (gh)^{1/2} = (2\pi^2 \rho h^2 G)^{1/2} \\ = \pi h \rho (2G/\rho)^{1/2}$$

This expression depends mainly on the mass  $h\rho$  of a unit sea area, but only weakly on the density  $\rho$  itself. As the assumption of the mass  $h\rho$  cannot be very wrong, the calculated wave velocity  $c$  using this formula will yield the correct order of magnitude.

Since the inner field is thin and dense, and the outer field is thick and much less dense, the value of  $c$  will be in the same order of magnitude for both the fields. If we suppose that the thickness  $h$  of the inner field is equal to 1/10 the radius of Mercury ( $0.038R_{\text{earth}} = 257$  km), and the masses of the four planets Mercury, Venus, earth and Mars are uniformly distributed over this field (outer radius = distance of Jupiter =  $778 \times 10^6$  km), the density of this field can be computed as follows:

$$(28) \quad \rho = \frac{M_{\text{earth}}}{\pi \times 778^2 \times 10^{12} \times 257} \\ = 1.23 \times 10^{-8} \text{ g/cm}^3$$

No correction about the gas masses blown

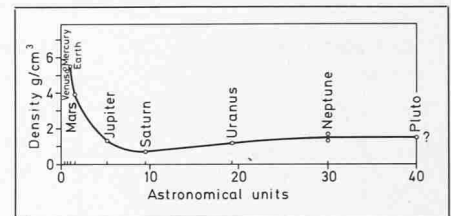


Fig. 12. Mean density of the planet

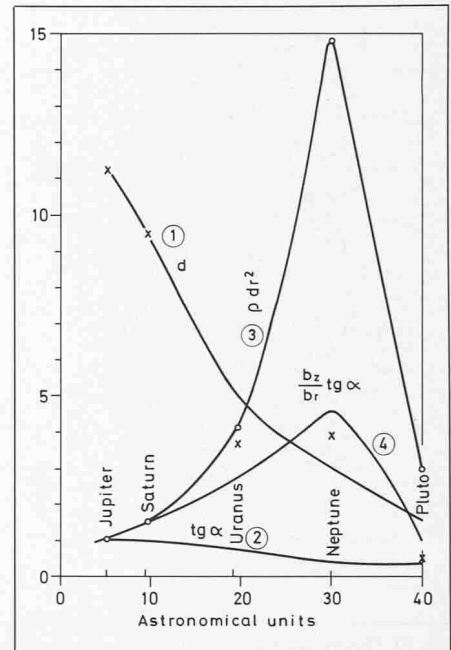


Fig. 13. Derivation of the correction term  $(b_z/b_r) \tan \alpha$  of Equation (21)

away by the T Tauri wind during the birth of the sun is made here.

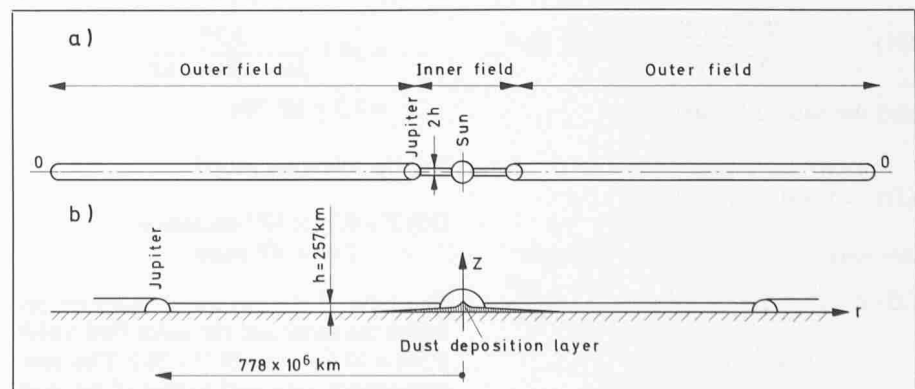
We obtain the travelling velocity of the tidal wave:

$$(29) \quad c = \pi \times 257 \times 10^5 \times 1.23 \times \\ 10^{-8} (2 \times 6.670 \times 10^{-8} / \\ 1.23 \times 10^{-8})^{1/2} \\ = 3.27 \text{ cm/s}$$

We suppose that this value applies to both the inner and the outer field. From  $c$  we

Fig. 14. A model for the primordial nebula disk of the solar system

- a) The nebula disk  
b) The circular sea transformed from the nebula disk





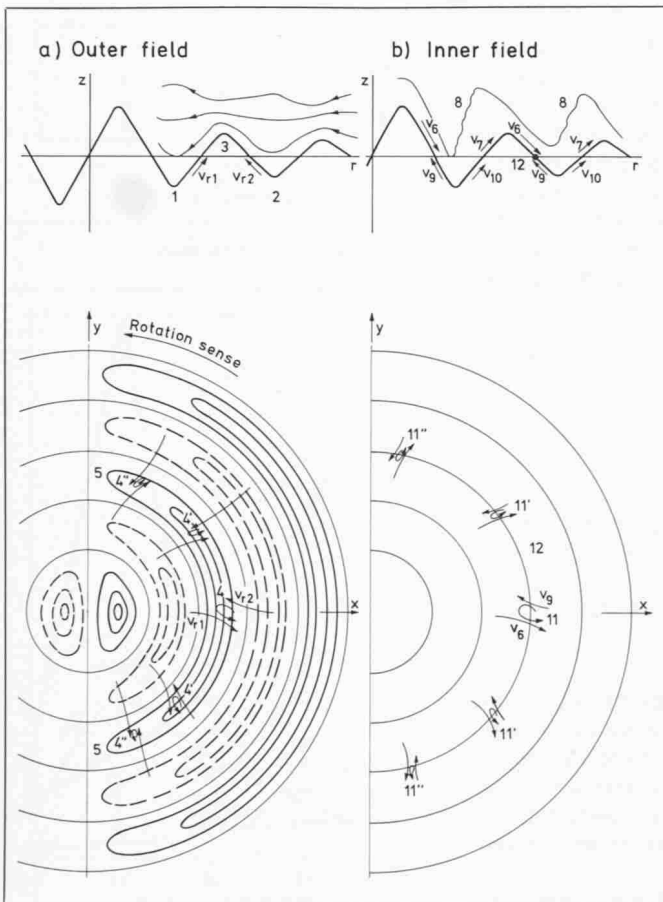
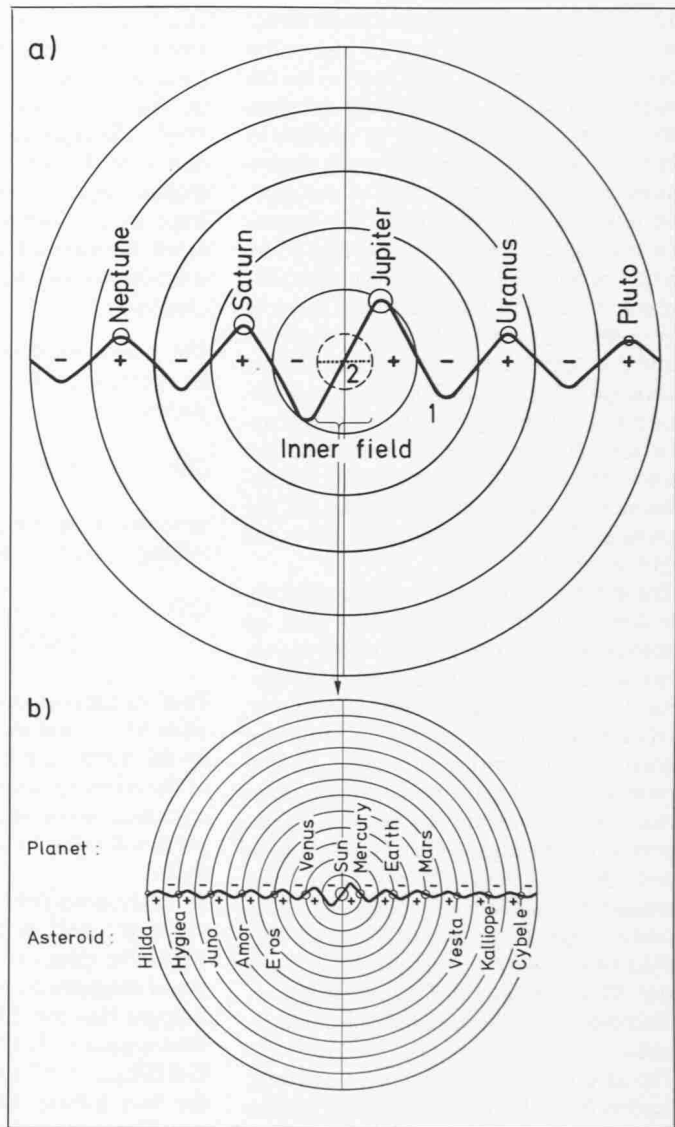


Fig. 15. Degeneration of the wave pattern to vortices due to Coriolis effect  
 a) in the outer field with formation of a vortex sheet 4-4'-4'' at a positive anti-nodal circle;  
 b) in the inner field with formation of a vortex sheet 11-11'-11'' at a nodal circle with downward surface wind  $v_6$

Fig. 16 (right). Distribution of the infant planetary vortices formed from the tidal waves

a) in the outer field b) in the inner field



can calculate the natural angular frequencies of the gaseous disk of the primordial solar system.

The parameter  $kr$  of the Bessel function  $J_0(kr)$  is 38.5 for the inner field extending to the asteroids of the Hilda Group (see Table 1), namely:

$$kr_{\text{Hilda}} = 38.5, \text{ where } r_{\text{Hilda}} = 583 \times 10^{11} \text{ cm}$$

$$(30) \quad \text{or } \frac{\omega r_{\text{Hilda}}}{c} = 38.5$$

therefore the natural angular frequency will be

$$(31) \quad \omega = \frac{38.5 \times 3.27}{583 \times 10^{11}} = 0.216 \times 10^{-11}$$

and the natural frequency

$$(32) \quad f = 0.0344 \times 10^{-11} = 0.344 \times 10^{-12} \text{ Hz}$$

We obtain the period of the vibration

$$(33) \quad T = \frac{1}{f} = 2.91 \times 10^{12} \text{ s} = \frac{2.91 \times 10^{12}}{31.5 \times 10^6} = 0.0925 \times 10^6 \text{ years} \\ (1 \text{ year} = 31.5 \times 10^6 \text{ s})$$

The vibration period is in the order of magnitude of a hundred thousand years for the inner field of the primordial gaseous disk.

For the outer field, the parameter  $kr$  is equal to 14.7 for

$$r = r_{\text{Pluto}} = 5904 \times 10^6 \times 10^3 \times 10^2 = 5904 \times 10^{11} \text{ cm (see Table 1)}.$$

We obtain the natural frequency:

$$(34) \quad f = 14.7 \frac{c}{2\pi r_{\text{Pluto}}} = 14.7 \frac{3.27}{2\pi \times 5904 \times 10^{11}} = 1.3 \times 10^{-14} \text{ Hz}$$

and the vibration period:

$$(35) \quad T = 0.77 \times 10^{14} \text{ seconds} = 2.44 \times 10^6 \text{ years}$$

The ratio of the natural frequencies between the inner and the outer field yields  $0.344 \times 10^{-12} / 1.3 \times 10^{-14} = 26.5$ . This ratio corresponds very well to that of the peak

frequencies of the energy densities between the two kinds of winds blowing over the corresponding two field (see previous chapter). We have thus proved the argument further again that the vibrations of the primordial gaseous disk of the solar system stay in a close relationship with its surface winds. Only this mutual interaction enables the coupling of these two elements to the self-excited vibration. In this manner, the existence both of the gaseous disk with its tidal wave pattern and of the surface winds blowing over it has been once more confirmed from the consideration of this mutual interaction.

Professor J. Wasserburg of the Institute of Technology in Pasadena, California, found from the difference in the ages between the meteorites fallen in Allende in Mexico in 1969 and the stones of the moon, that the formation of the solar system would take a time of about  $100 \cdot 10^6$  years.

According to the calculation of R. B. Larson 1969, an interstellar sphere-shaped cloud of a size of  $5 \cdot 10^6$  times the sun and a mass of the sun would require a duration of about  $0.5 \cdot 10^6$  years first for its contrac-

tion into the spherical infant solar system and then for its further development to the final form. His spheric model deviates considerably from our disk-shaped one. Nevertheless, his result provides us a useful clue for the estimation of the time for the contraction of the primeval cloud to our primordial gaseous disk. We may estimate that this time would amount to the order of magnitude of  $10^6$  years. This is really negligible to the time of  $100 \cdot 10^6$  years available for the complete formation of the solar system. Then practically, this whole time would stay at our disposal for the further development of the primordial gaseous disk. Let us suppose that half this time would be needed for the growth of the vibrations in the gaseous disk. Then we could infer that the inner and the outer planet field would survive about 500 and 20 cycles of the vibrations, respectively, until their amplitudes would grow so great that they would be disintegrated into vortices due to the non-linear effect mentioned previously. The vortices would take the rest of the time available for their evolution to the sun, the planets and the asteroids.

The wave pattern of the outer field is shown in Fig. 16a by curve 1, and that of the inner field is shown by points 2 (as well as in an enlarged scale in Fig. 16b). The circles denote the nodal circles for the inner field, and for the outer field. As already compiled in Tables 1 and 2, the planets and the asteroids are formed either on these circles (inner field) or in between (outer field). Actually, the wave of the outer field extends into the inner field (see Fig. 16a), despite the fact that the thickness and the density of the inner field are different from those of the outer field. As is well known for a gas flow through a circular cylinder, its natural frequency and its vibration pattern over the circular crosssection will not be influenced very much, when there is a second cylinder of a very small diameter inserted co-axially and concentrically into the original one.

We therefore have a superposition of two waves in the inner field, one with a long wavelength as an extension from the outer field and the other one with a considerably short wavelength due to its own natural vibration of the inner field. These two waves are entirely decoupled due to the great difference in their wavelengths.

The *Bessel function* given in Fig. 3 predicts a decrease of the wave amplitude with the increase of the radius  $r$ , see Figs. 16a and 16b. This phenomenon correspond very well to the general tendency of the decrease of the planet size with the distance from the sun, with the only exception of Mercury. Does this mean that the primordial nebula around it has been pulled away by the sun due to its great gravitation force?

The wave pattern of the inner field does

not reach the border of Jupiter. It ends at the asteroids of the *Hilda Group*. The transition zone from the outer border of the inner field to the inner border of the outer field, i. e. between the asteroids Hilda Group and Jupiter, has a width of a quarter of the radius of Jupiter from the sun. It seems that the gas in this zone of the primordial gaseous disk streamed to Jupiter contributing to its formation. This will be discussed furthermore in some details in a following part.

An examination of the question will be carried out about whether the primordial gaseous disk of the solar system were dense enough as to be considered as a fluid-dynamic system.

The temperature of the primordial gaseous disk can be supposed to be in the range of 10 Kelvin. If we suppose that the content of the disk is entirely molecular hydrogen, the pressure in the disk will be

$$\begin{aligned} p &= \rho RT \\ &= 1.23 \times 10^{-8} \times 420.75 \times 10 \\ (36) \quad &= 0.52 \times 10^{-8} \text{ bar} \end{aligned}$$

The molecule number of hydrogen in  $1 \text{ cm}^3$  will be

$$\begin{aligned} n &= \frac{\rho}{m} \quad (m = \text{mass of a} \\ &\quad \text{hydrogen molecule}) \\ &= \frac{1.23 \times 10^{-8} \times 10^{-6}}{3.35 \times 10^{-27}} \\ (37) \quad &= 0.367 \times 10^{13} \end{aligned}$$

The mixture length:

$$\begin{aligned} l &= \frac{1}{2^{1/2} n \pi \delta^2} \quad (\delta = \text{effective diameter} \\ &\quad \text{of a hydrogen molecule}) \\ (38) \quad &= \frac{1}{1.41 \times 0.367 \times 10^{13} \times \pi (2.72 \times 10^{-8})^2} \\ &= 83 \text{ cm} \end{aligned}$$

molecular velocity

$$(39) \quad c = (3 RT)^{1/2} = 352 \text{ m/s}$$

Impact number per second:

$$(40) \quad \frac{c}{l} = \frac{352}{0.83} = 425$$

The treatment of the primordial gaseous disk as a fluid system using the fluid dynamic laws can thus be proved to be adequate.

### Development of the solar system from vortices of the primordial gaseous disk

As shown in the previous chapters the transformed potential vortex field is invis-

cid which provides the primordial solar gas disk with an ideal property as if its viscous effect were blocked. The gas disk could then perform vibrations without resistance from the damping.

However, this ideal property will remain so long as the disturbances in the linear distribution of the circulations arising from the vibrations are small. Therefore, the gas system as a vibrating disk can only be sustained at small amplitudes. If the amplitudes become great, the ideal condition breaks down. Then the linear approach of the circulation distribution is no longer valid. The gas system retains its real property with viscosity again. Vortices can be generated and grow with time.

In a usual rotating gaseous disk which does not possess the condition of a potential vortex, every point has its own local vorticity  $\omega$ :

$$(41) \quad \omega = 1/2 \left( \frac{v_\varphi}{r} - \frac{\delta v_\varphi}{\delta r} \right)$$

For a general rotating gaseous disk possessing the following rotating curve (i. e. the distribution of the swirl velocity  $v_\varphi$  over the radius  $r$ ):

$$(42) \quad r^n v_\varphi = \text{const} = k,$$

the derivation yields

$$(43) \quad \omega = 1/2 (1-n) \frac{k}{r^{n+1}}$$

with  $n = 1/2$  for the solar system, we obtain

$$(44) \quad \omega = 1/4 \frac{k}{r^{3/2}}$$

This angular velocity has the same sense of the rotation of the gaseous disk. We can easily prove that  $\omega = 0$  for a potential vortex because of  $n = 1$ .

If the approach of the rotating curve of the primordial gaseous disk of the solar system with local potential vortices, as carried out in a previous chapter, is no longer valid, then this disk will possess a local angular velocity increasing with the decrease of the radius in accordance with eq. (44). The local angular velocity is very great in the central region and very weak in the outer edge. The loss of the state of the potential vortex will take place, when the wave pattern of the gaseous disk becomes very strong and thus strong radial fluctuating velocities arise due to the vibration. The orbit of a gas particle will be strongly elliptical, deviating largely from the circular path (see Figs. 16a & 16b), a strong violence to the precondition of the approach mentioned. Then, the Coriolis acceleration  $2\omega v_r$  accompanied with the local angular velocity must be considered.

The wave pattern of the gaseous disk is sketched in Fig. 15a and b. The ridges of the wave are drawn with full lines and its furrows are drawn with dotted lines. The peaks and the valleys lie along the x-axis.

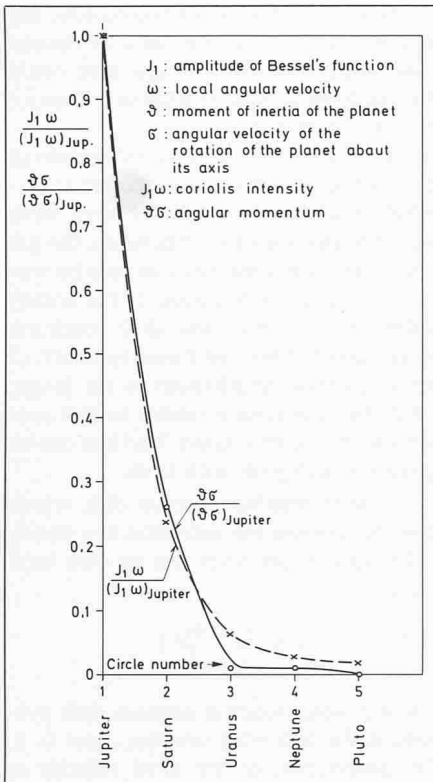


Fig. 17. Comparison between the angular momentum of the planet at the present stage and the coriolis intensity of the primordial nebula disk of the solar system

For the outer field with a mild wind over the wave pattern, as shown in Fig. 11g, the radial particle velocity  $v_r$  of the wave motion will be deflected rightward due to this Coriolis force. This is shown in Fig. 15a for two radial flows coming from the valleys 1 and 2 along the two flanks of the peak 3. As the wind is symmetrical on these two flanks, the two radial flows will possess equal radial velocities  $v_{r1}$  and  $v_{r2}$ . Due to their deflection, a strong vortex 4 with the same rotation sense of the rotating disk will be generated. Similarly, weaker vortices 4' and 4'' will be formed in the weaker wave regions along the ridge of wave due to their smaller radial velocities and then their smaller deflection. We thus have a vortex sheet along this ridge, whose intensity increases from its foot 5 to its peak 4. This vortex sheet will then develop to a concentrated vortex at the peak of the ridge.

The situation in the inner field is somewhat different. It is argued in Fig. 11f that the velocity of the wind downward from the ridge ( $v_6$  in Fig. 15b) can be very strong, but that upward from the furrow,  $v_7$ , can be very weak. The shock front is denoted by 8.

It is thus to be expected that the strong wind 6 is a main controlling factor for the flow field. The vortex sheet 11 formed by the wind  $v_6$  and the vibrating velocity  $v_9$  at the nodal circle 12 can be considered to be the primary vortex field, which will then finally develop to a concentrated vortex. The vortex model shown in Fig. 15 yields

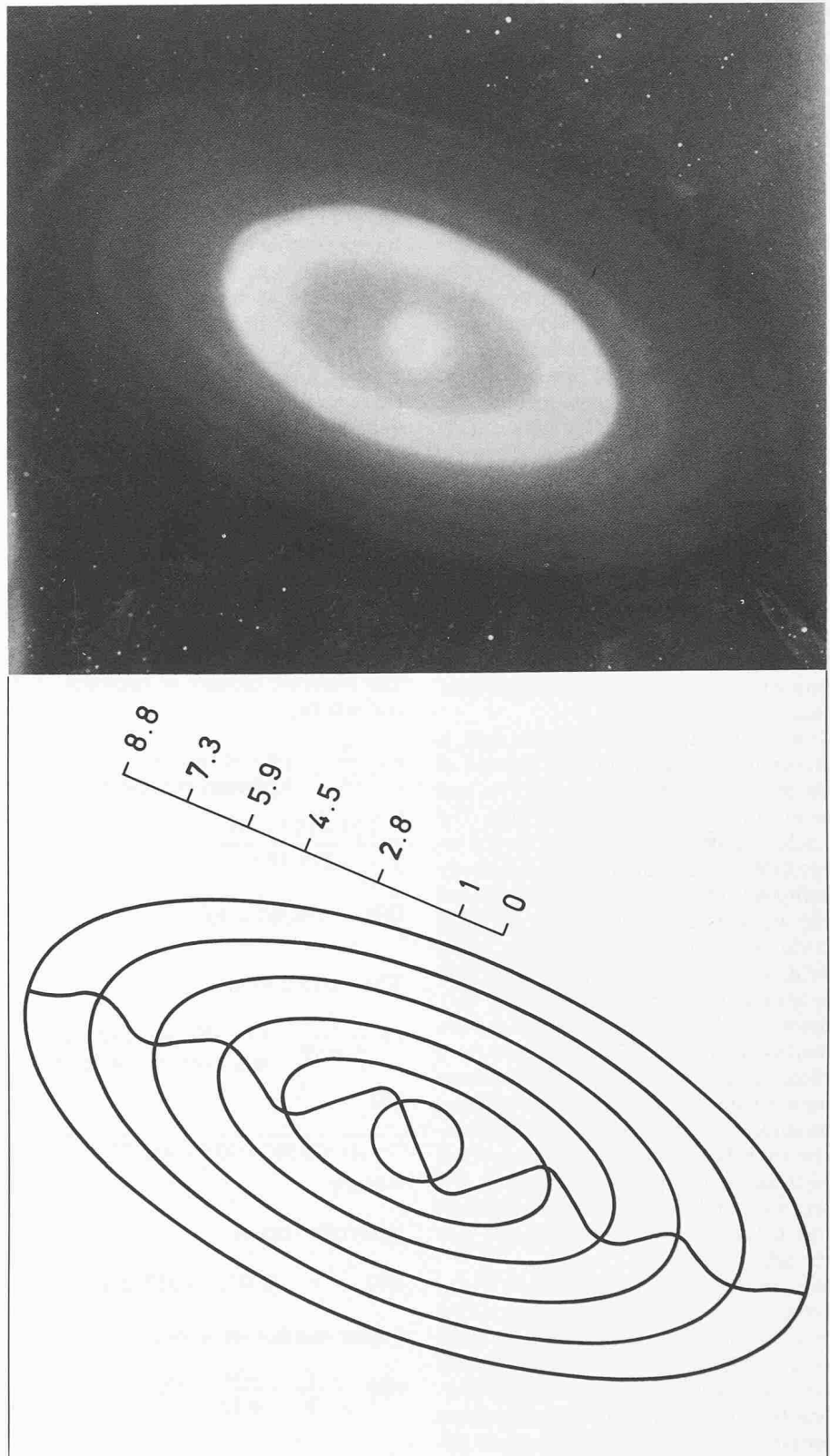


Fig. 18. Birth of a planetary system of a disk shape observed by American astronomers in the constellation of Cygnus (NASA drawing, see Hahn 1978)

the formation of the vortices at the positions of the peaks of the wave pattern for the outer field, but at the nodal circles situated at the downhill side of the surface wind for the inner field. As we have a wave pattern with a nodal diameter, the vortices will be formed alternately on the two sides of the nodal diameter. The distributions of these vortices are shown in Fig. 16a for the

outer field and in Fig. 16b for the inner field. The vortices are designated with the names of the planets and the asteroids, into which they will be finally converted.

It is to be expected that the intensity of the vortex, which is formed by the radial velocity of the wave field  $v_r$  and the local angular velocity  $\omega$  as for the case of the outer field, must be proportional to the product



of the amplitude of the *Bessel function*  $J_1$  given in Fig. 3 and the local angular velocity  $\omega$  being proportional to  $r^{-3/2}$  (eq. 44). On the other hand, the angular momentum  $\sigma$  of the planet ( $\sigma$ : moment of inertia of mass,  $\sigma$ : angular velocity of the planet about its rotating axis) as the final stage of the development of the vortex must be comparable with the product  $J_1\omega$ . The calculated result of these two expressions, normalized by the corresponding values for Jupiter, are plotted over the circle number, i. e. the position of the planet, in Fig. 17. A reasonable agreement between the two curves is obvious. This result yields a further confirmation of the theory developed in the present paper.

In this consideration, only the coriolis term  $J_1\omega$  of the primordial gaseous disk is taken. No further effort is made to include the mass term, because the property of the vortex of the infant planet cannot be derived from this simplified theory. This refinement must be left for the future. A similar task for the inner field as that in Fig. 17 cannot be carried out because the dominating velocity here is the velocity of the surface wind, but not that of the wave field. This wind velocity cannot yet be modelled for the present.

The *asteroids* lie in the outer edge of the inner group. Their circulations deviate largely from the straight line, approaching the distribution of the circulations of the group (Fig. 1a). Thus, the flow field of the asteroids deviates somewhat from the potential vortex, applied to the other planets covered by this group. Therefore, a certain degree of damping will occur in the wave pattern in this region due to the non-ideal distribution of the swirl velocities. Local turbulence cells will be generated by the differentially revolving orbits of the gaseous medium, as a result of the shear of the neighbouring layers. The turbulence cell will lock the heavy particles carried with it and cause these to form into a larger congregation. The tidal waves of the gas disk, weakened by the turbulent activity can no longer be capable of producing vortices with sufficient intensities. This will result in the failure in the formation of the planets from the numerous turbulent cells of the gaseous disk. Nevertheless, the wave pattern is still conserved in the belts of the asteroids formed from these turbulent cells which are kept separate by the *Kirkwood gaps*. The middle circles of these belts correspond very well to the nodal circles of the theoretical wave pattern (see Fig. 16b).

It is to be noticed that only an asteroid group (Eros) has been formed between earth and Mars (see Fig. 16). The failure in the formation of a planet in this belt could be explained using the flow model sketched in Fig. 11. The corresponding belt would have coincided with the thinnest part of the primordial nebula disk

caused by the compression of the inflow 3, as proposed in Figs. 11b and 11d. This part would have been very turbulent because of the frontal impact of the surface winds 5 from both sides of the disk. This strong turbulence would have caused the formation of the asteroid group mentioned instead of a planet much the same as for the asteroids between Mars and Jupiter. As the flow field in this part of the nebula disk would have deviated much from the normal one upstream of this surface wind, the orbit of the following planet Mars departs thus somewhat from the theoretical pattern as shown in Fig. 5.

### The observations made in the space

H. M. Hahn reports in his book, 1978, two direct observations out of the space, which strongly support the flow model developed in the present paper. One of the observations was made by E. Erickson and F. Wittborn (Kniper Airborne Observatory) as well as R. Thompson and P. Strittmatter (Steward Observatory of the University of Arizona). They found a disk-like cloud of gas and dust surrounding a developing star in the constellation of Cygnus. A drawing performed by NASA is given in Fig. 18. It is estimated that the star has a mass of about  $30M_{\odot}$ , a radius of about 8 times the radius of the sun and a surface temperature of about 40 000 Kelvin. The outer edge of the disk is estimated to be beyond the orbit of Pluto of our solar system, and its gleaming inner core to have a radius of larger than the distance sun-earth. As shown in Fig. 18, the disk cools down outward. The scientists believe that the gleam of the inner core is caused by the friction heat generated by the steady impact of the particles flowing into this region. This could be interpreted to be the jet-like in-

flow in our fluid-dynamic model (Fig. 11b).

Let us suppose that the edge between the neighbouring annular rings representing two different temperature fields in Fig. 18 would indicate a change of the direction of the disk surface which radiates the heat to supply the temperature measurement. Then we could interpret that the circular edge between any two differently coloured annular rings of Fig. 18 would represent a ridge or a furrow circle of the tidal wave pattern, as sketched in Fig. 18. As the intensity of this wave increases inward, the amplitude and the temperature will increase correspondingly, as observed by the scientists cited above. The radii of the ridge or the furrow circles are measured from the figure and shown on the wave pattern, whereby the radius of the innermost ridge circle is chosen as unity. The value of the radius of the circle can then be read off and plotted in Fig. 19 as curve 1 with the circle number as abscissa. The theoretical curve, as denoted by curve 2, represents the ideal tidal wave pattern applied to the outer field of the solar system (i. e. from Jupiter to Pluto). The fact, that curve 2 agrees very well with curve 1, is extremely encouraging for our theory about the primordial gas disk of the solar system.

Thus, we discover a forming planetary system of a disk-like shape in the space, exhibiting the same tidal wave pattern in its outer field as the one predicted by the present theory for the primeval gas disk of our solar system. An inward blowing surface wind must therefore also prevail over the planetary disk discovered, producing this wave pattern. There must be also likely an inner planet field present in this system, but it is hidden by the luminescent light of the inner core.

It is to be noted that a dark blue semicircle can be detected at the position of the inner-

Fig. 19. Comparison of the temperature field of the planetary disk given in Fig. 18 with the wave pattern of a usual gaseous disk

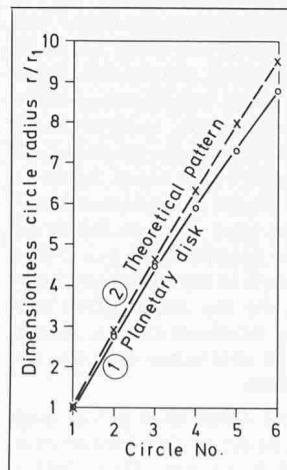
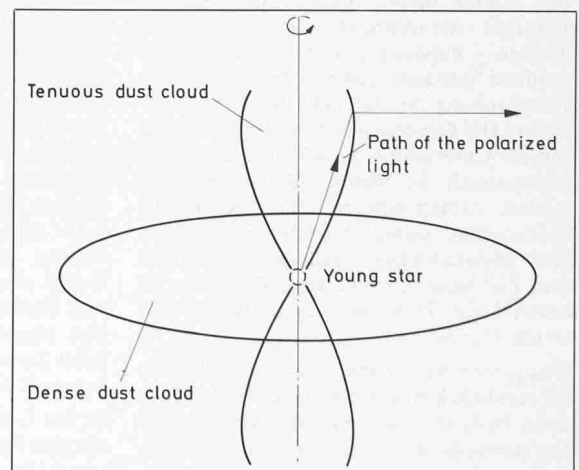


Fig. 20. Deflection of light by jet-like central flow of a star at the formation stage surrounded by a nebula disk (Max-Planck-Institute for Astronomy at Calar Alto in South Spain, see Hahn 1978)



most ridge. Does it represent the impact front of the two surface winds, one from the outer zone inward and the other from the center outward, as argued in our flow model of Fig. 11? The diameter through the gas disk limiting this semicircle would indicate the nodal diameter of the tidal wave pattern as predicted by the theory. The second observation was revealed by A. Schulz, Th. Schmidt and K. Proetel of the Heidelberg Max Planck Institute for

Astronomy. They likewise discovered a planetary dense gas disk in the constellation of Cassiopeia. They found a jet-like cloud over the polar region of the forming star situated at the center of the disk, as sketched in Fig. 20. The light radiated by the star will be polarized and deflected by this jet-like cloud to the direction of the observers.

The two series of observations quoted previously supply, thus, further confirmation

of the theory for the existence of a primordial gas disk of the solar system. These direct measurements supply a really welcome evidence for the adequacy of the theory developed.

**Part III: "Derivation of the Behaviours of the Sun and the Planets" in the next issue of this journal (27.1.83).**

The authors' address: Dr. Y. N. Chen, dipl. Ing. ETH, Gebr. Sulzer, Aktiengesellschaft, CH-8401 Winterthur.

## Umschau

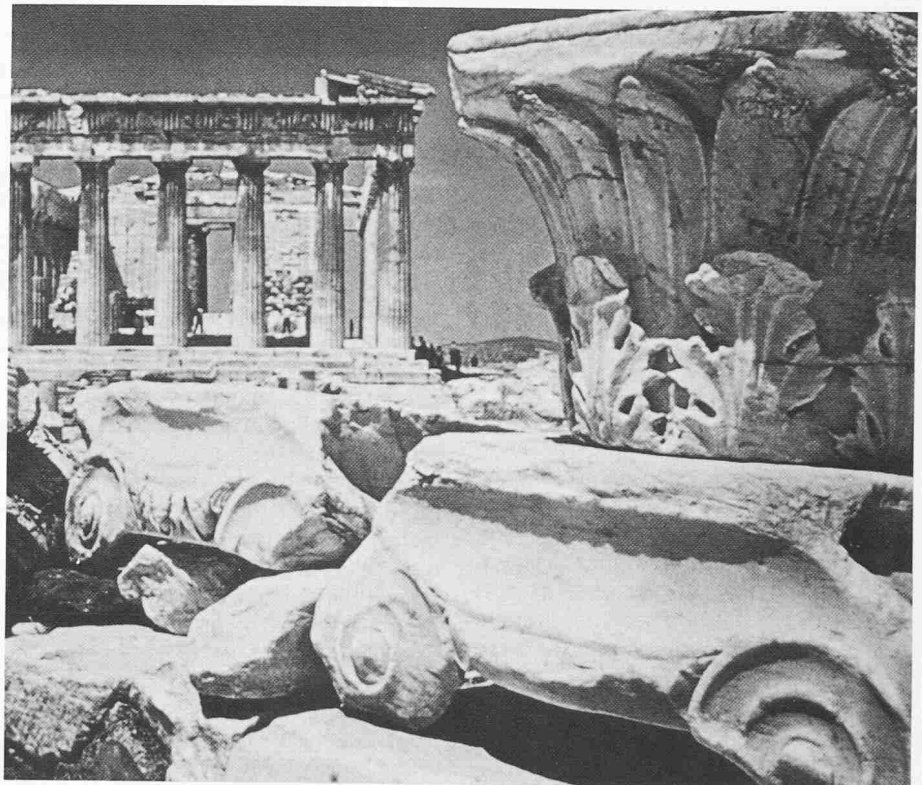
### Kultur und Technik – zwei voneinander unabhängige Welten?

(up). Der erste Vortrag im neuen Jahr für die Mitglieder des *Technischen Vereins* und des *SIA Winterthur*, gehalten von Technorama-Direktor Dr. S. Aegerter, befasste sich mit dem Thema «Kultur und Technik». Schon zur Begrüssung wies Vereinspräsident U. Isler die interessierte Zuhörerschaft auf die besondere Mittlerfunktion des Technoramas hin. Seine Bemerkung, das Technorama habe auch weiterhin «ausserplanmässige» finanzielle Unterstützung nötig, wird sicher in die richtigen Ohren gelangt sein.

Zwei verschiedene, offenbar voneinander unabhängige intellektuelle Welten bestimmen unser Leben: die *humanistische* und die *technische*. Denn, so Simon Aegerter, wenn man von Kultur und Technik spricht, so sind damit offenbar *zwei verschiedene Dinge gemeint*, zwei Betrachtungsweisen, sogar zwei Sorten Menschen. Ein gebildeter Mensch kennt die Weltliteratur in Wort und Ton, er kann ein Andantino von einem Menuett unterscheiden, er ist in der griechischen Götterwelt ebenso zu Hause wie bei den Geliebten Goethes. Wer jedoch imstande ist, Differenzialgleichungen zu lösen, Computerprogramme zu schreiben, wer den thermischen Wirkungsgrad erklären oder eine Kaplan- von einer Pelton turbine unterscheiden kann, der ist nicht gebildet, sondern höchstens ausgebildet. Er taugt nicht als Konversationspartner, er ist technokratenverdächtig.

Wie könnte dieser *Graben* zwischen den Kulturen – der technischen und der humanistischen – entstanden sein, welche Folgen hat diese Spaltung, und welche Chancen zur Überwachung des Grabens bestehen überhaupt? Die Geisteswelt der *Griechen* kannte keinen Unterschied zwischen Kultur und Wissenschaft. Im Weltbild der Pythagoräer spielten Zahlen eine besondere Rolle. Die Philosophen waren Naturwissenschaftler. Ihre physikalischen Entdeckungen haben zum Teil heute noch Gültigkeit. Aber – sie waren keine Technokraten, sie waren *Kulturschaffende*!

Was jedoch hat zwischen damals und heute die parallele Entwicklung dieser beiden Kulturen bewirkt? Aegerter vermutet, dass die *Dogmentreue der mittelalterlichen Geisteswelt* ein wesentlicher Anteil an dieser Ent-



Unterschiedliche Betrachtungsweise von Kulturschaffenden und Technikern: Der eine sieht hier ein korinthisches Kapitäl der andere einen Verwitterungsprozess?

wicklung hatte. Das den Menschen damals zugängliche Wissen galt als vollständig, neue Ideen waren verpönt, forschende Neugier wider die göttliche Allmacht. Da musste sich die Naturwissenschaft gezwungenermassen im *Untergrund* entwickeln, musste sich abkapseln vom übrigen Geistesleben. Aus diesem *Ghetto* sind Naturwissenschaftler und Ingenieure im Grunde nie mehr herausgekommen. Im Gegenteil: Naturwissenschaftler bilden heute einen weitgehend geschlossenen Kreis mit eigener, für Aussenstehende kaum verständlichen Sprache. Sie denken in abstrakten Modellen und haben Wertordnungen, die von denen der «grossen Mehrheit» verschieden sind. Und sie haben ein Wissen, das der grossen Mehrheit Angst macht. *Angst jedoch ist ein schlechter Ratgeber*. Entscheide, die aus Angst gefällt werden, neigen dazu, irrational zu sein. Irrationales Verhalten ist aber genau das, was wir heute oft beobachten:

In der Geschichte dieser Erde gab es noch nie eine Epoche, in der so viele Menschen so gut gelebt haben. Es ist ganz offensichtlich,

dass dieser weitverbreitete Wohlstand nur dank der Technik möglich ist. Trotzdem konnte in der westlichen Welt eine Bewegung entstehen, welche die noch vorhandenen Probleme und die im Zusammenhang mit Problemlösungen neu auftauchenden Probleme ausschliesslich der Technik anlastet und daraus die Forderung nach ihrer Abschaffung oder mindestens Reduktion herleitet. Wir drücken heute Knöpfe und selbstverständlich setzt ein, was wir erwarten: Licht, Wärme, Musik, Kommunikation. Die *sofortige Erfüllung materieller Bedürfnisse auf Knopfdruck* ist derart selbstverständlich geworden, dass man sich auch nach der Erfüllung höherer Werte sehnt: nach *Liebe, Geborgenheit, Verständnis, Anerkennung*. Lastet man der Technik an, dass sie hierzu keine Druckknöpfe erfinden kann?

Es ist Mode geworden, aus der Welt der Technik auszusteigen, sich eine eigene Welt zu schaffen, eine Welt, in der man nur nach Höherem strebt. Man fordert Abkehr von der Grosstechnik, vom Materialismus, vom